# A COMPARATIVE STUDY OF FINITE VOLUMES, FINITE DIFFERENCES AND MESHLESS METHODS FOR DRIVEN CAVITY PROBLEM

**José Laércio Doricio**
SEM-EESC-USP
josedoricio@yahoo.com.br

**Antônio Carlos Henriques Marques**
SEM-EESC-USP
achm@sc.usp.br

**Marcelo Yutaka Noguti**
CCNE - UFSM
mfnoguti@terra.com.br

***Abstract.*** *The aim of this study is compare Finite Volumes, Finite Differences and Meshless methods applied to the classic problem of the square driven cavity. In the three methods it was used the MAC (Marker-And-Cell) methodology, structured mesh to Finite Differences and unstructured mesh to Finite Volumes. The necessary points to Meshless method were obtained from the computational nodes generated by Finite Volumes mesh. The effect of the numeric viscosity was compared with the results obtained with the known classic results of the Finite Differences method applied to cavity problem. In Finite Volumes method it was used cell centered for the velocity field* $\mathbf{u}$ *and pressure* $p$*, and the convergence was accelerated through the Bi-conjugated Gradient Stabilized method. In the Meshless method, it was used the exponential weight function and Least Square method. In all methods it was adopted the primitive variables and for simulations it was used Reynolds numbers equal to 0.1, 10, 50 and 100. Interesting characteristics of the flow are presented in details - the velocity field to central lines and the streamlines. The formulation is second order in spacial variables and explicit of first order in time variables.*

***Keywords:*** *Finite Volumes, Finite Differences, Meshless, Primitive Variables, Numerical Simulation.*

## 1. Introduction

The driven cavity flow has been studied very extensively and is possible to find many papers about this flow problem in the literature. Driven cavity flow serves as a benchmark problem and almost every new numerical method for the 2-D steady incompressible Navier-Stokes equations are tested on the driven cavity flow in terms of accuracy, numerical efficiency, boundary conditions, etc. Among many numerical studies on driven cavity flow it can be cited Erturk et al. (2004), Barragy and Carey (1997), Schreiber and Keller (1983), Benjamin and Denny (1979), Ghia et al. (1982). To solve the stationary incompressible Navier-Stokes equations in the square driven cavity problem it was employed three methods: the Finite Volumes method, to solve problems of unstructured meshes, see Maliska (2000), Maliska and Vasconcellos (2000), Schneider and Maliska (2000, 2002); the Finite Differences method, that is a classic method used to solve problems involving the driven cavity, see Fletcher (1991), Maliska (2000), Semeraro and Sameh (1991), Versteeg and Malalasekera (1995); and the Meshless method, that is an alternative method to eliminate the mesh of the problem, see Belytschko et al. (1996), Melenk (1997), Choe et al. (2001), Günter and Liu (1997). The main purpose of this study is compare Finite Volumes, Finite Differences and Meshless methods applied to the driven cavity problem in terms of numerical accuracy and boundary conditions. The Navier-Stokes incompressible equation and the MAC methodology were used by all formulations. Low and moderated Reynolds numbers ($Re$=0.1, 10, 50 and 100) were tested. Based on the results obtained, a brief discussion about the physical, mathematical and numerical nature of a 2-D driven cavity will be done.

## 2. Problem Formulation, Basic Equations and Discretizations

It was seeking a steady solution of an incompressible flow in a bi-dimensional square driven cavity. It was used the incompressible Navier-Stokes to solve the driven cavity flow problem. For the Finite Differences and Meshless methods it was used the differential formulation of basic equations. For the Finite Volumes method it was used the integral formulation of the governing equations. A solution for the equation system of incompressible Navier-Stokes can be made by two very common strategies: using the vorticity stream-function approach or the primitive variable approach. In this study, it was adopted the primitive variable approach. The differential formulation for the bi-dimensional incompressible Navier-Stokes is given by:

$$\left.\begin{aligned}&\frac{\partial u}{\partial t}+u\frac{\partial u}{\partial x}+v\frac{\partial u}{\partial y}=-\frac{\partial p}{\partial x}+\frac{1}{Re}\left(\frac{\partial^2 u}{\partial x^2}+\frac{\partial^2 u}{\partial y^2}\right)\ ,\\&\frac{\partial v}{\partial t}+u\frac{\partial v}{\partial x}+v\frac{\partial v}{\partial y}=-\frac{\partial p}{\partial y}+\frac{1}{Re}\left(\frac{\partial^2 v}{\partial x^2}+\frac{\partial^2 v}{\partial y^2}\right)\ ,\\&\frac{\partial u}{\partial x}+\frac{\partial v}{\partial y}=0\end{aligned}\right\}\tag{1}$$

where $Re$ is the Reynolds number defined as $Re=\frac{\rho U_\infty L_\infty}{\nu}$, $\rho$ is the density of the fluid, $U_\infty$ and $L_\infty$ are lenght and velocity characteristic of the flow, $\nu$ is the viscosity of fluid; $\mathbf{u}=(u,v)$ is the velocity field; and $p$ is the pressure field. The integral formulation is given by Eq. (1) integrated in the control volume $V$, then Green's Theorem was applied resulting in:

$$\left.\begin{aligned}&\frac{\partial u}{\partial t}=-\frac{1}{V}\int_V\frac{\partial p}{\partial x}dV+\frac{1}{V}\oint_S\left[\left(\frac{1}{Re}\frac{\partial u}{\partial x}-u^2\right)dy-\left(\frac{1}{Re}\frac{\partial u}{\partial y}-uv\right)dx\right]\ ,\\&\frac{\partial v}{\partial t}=-\frac{1}{V}\int_V\frac{\partial p}{\partial y}dV+\frac{1}{V}\oint_S\left[\left(\frac{1}{Re}\frac{\partial v}{\partial x}-uv\right)dy-\left(\frac{1}{Re}\frac{\partial v}{\partial y}-v^2\right)dx\right]\ ,\\&\int_V\left(\frac{\partial u}{\partial x}+\frac{\partial v}{\partial y}\right)dV=0\end{aligned}\right\}\tag{2}$$

Different methods have been employed for the solution of the incompressible Navier-Stokes equations system expressed in primitive variable form. The Meshless and the Finite Differences methods are solved using the Eq. (1) and the Finite Volumes by Eq. (2) through the MAC algorithm, see Harlow and Welch (1965). It can be supose that the velocity field $\mathbf{u}(\mathbf{x},t_n)$ is known and boundary conditions for velocity and pressure are given. The velocity and pressure fields at time $t=t_n+\delta t$ are calculated as follows:

Let $\widetilde{p}(\mathbf{x},t_n)$ be a pressure field. Inserting $\widetilde{p}(\mathbf{x},t_n)$ into Eq. (1) it is compute a tentative velocity field $\widetilde{u}(\mathbf{x},t_n)$ from

$$\left.\begin{aligned}&\frac{\partial \widetilde{u}}{\partial t}+u\frac{\partial u}{\partial x}+v\frac{\partial u}{\partial y}=-\frac{\partial \widetilde{p}}{\partial x}+\frac{1}{Re}\left(\frac{\partial^2 u}{\partial x^2}+\frac{\partial^2 u}{\partial y^2}\right)\ ,\\&\frac{\partial \widetilde{v}}{\partial t}+u\frac{\partial v}{\partial x}+v\frac{\partial v}{\partial y}=-\frac{\partial \widetilde{p}}{\partial y}+\frac{1}{Re}\left(\frac{\partial^2 v}{\partial x^2}+\frac{\partial^2 v}{\partial y^2}\right)\ ,\end{aligned}\right\}\tag{3}$$

with $\widetilde{\mathbf{u}}(\mathbf{x},t_n)=\mathbf{u}(\mathbf{x},t_n)$ using the appropriate boundary conditions for $\widetilde{\mathbf{u}}(\mathbf{x},t_n)$ at $t=t_n$. The Eq. (3) is solved by a Meshless method or by an explicit Finite Differences method. Let $\mathbf{u}(\mathbf{x},t_n)$ be defined by

$$\mathbf{u}(\mathbf{x},t)-\widetilde{\mathbf{u}}(\mathbf{x},t)=-\nabla\psi(\mathbf{x},t)\tag{4}$$

where $\psi(\mathbf{x},t)$ is a function having the property

$$\nabla^2\psi(\mathbf{x},t)=\nabla\cdot\widetilde{\mathbf{u}}(\mathbf{x},t)\ .\tag{5}$$

Thus, $\mathbf{u}(\mathbf{x},t_n)$ conserves mass and the correct vorticity at time $t$. An equation for pressure is obtained as follows. By subtracting Eq. (1) from Eq. (3) it can be write

$$\frac{\partial\mathbf{u}-\widetilde{\mathbf{u}}}{\partial t}=-\nabla(p(\mathbf{x},t)-\widetilde{p}(\mathbf{x},t_n)).\tag{6}$$

Now, introducing Eq. (4) into Eq. (6) it yields

$$-\frac{\partial\nabla\psi(\mathbf{x},t)}{\partial t}=-\nabla(p(\mathbf{x},t)-\widetilde{p}(\mathbf{x},t_n)).\tag{7}$$

and interchanging the operators in Eq. (7) it's obtained $p(\mathbf{x},t)=\widetilde{p}(\mathbf{x},t)+\frac{\partial\psi(\mathbf{x},t)}{\partial t}$, which is evaluated as

$$p(\mathbf{x},t)=\widetilde{p}(\mathbf{x},t)+\frac{\psi(\mathbf{x},t)}{\delta t}\ .\tag{8}$$

Therefore, for simulating the flow it can solve the equations Eq. (3), Eq. (5), Eq. (4) and Eq. (8), respectively. The derivatives in the Finite Differences were calculated using the second order approximation and the convective terms were calculated using the second order upwind method VONOS, see Varonos and Bergeles (1998). To calculate the derivatives in the Meshless method was used the formulation of Franke and Nielsen. Let

$$V_I(\mathbf{x}) = c_1(x - x_I)^2 + c_2(x - x_I)(y - y_I) + c_3(y - y_I)^2 + c_4(x - x_I) + c_5(y - y_I) + c_6 \ .$$

It can be observed that when $\mathbf{x} = I$ then $c_6 = V_I$. To determinate the values of $c_1, ..., c_5$ can be used the Least Square method. Let:

$$\xi = x - x_I \ , \qquad \eta = y - y_I \ , \qquad V_I(\mathbf{x}) = f \ , \quad \Rightarrow \qquad f(\xi, \eta) = c_1\xi^2 + c_2\xi\eta + c_3\eta^2 + c_4\xi + c_5\eta \ . \tag{9}$$

By the Least Square method $\wp(\mathbf{x}) = g_1\alpha_1 + g_2\alpha_2 + g_3\alpha_3 + g_4\alpha_4 + g_5\alpha_5$ and comparing with Eq. (9) it can be saw that

$$g_1 = \xi^2, \qquad g_2 = \xi\eta, \qquad g_3 = \eta^2, \qquad g_4 = \xi, \qquad g_5 = \eta \ .$$

Than it needs to solve the system $\mathbf{Ac} = \mathbf{b}$ to find values for the constants $c_1, ..., c_5$:

$$A_{ij} = \sum_{k=1}^{m} g_j(x_k)g_i(x_k) \ , \qquad b_i = \sum_{k=1}^{m} f(x_k)g_i(x_k) \ . \tag{10}$$

where $m$ is the number of neighbors of $I$, according to Fig. 1 c. Expanding Eq. (10) is had:

$$\mathbf{A} = \begin{bmatrix} <\xi^2,\xi^2>_k & <\xi^2,\xi\eta>_k & <\xi^2,\eta^2>_k & <\xi^2,\xi>_k & <\xi^2,\eta>_k \\ <\xi\eta,\xi^2>_k & <\xi\eta,\xi\eta>_k & <\xi\eta,\eta^2>_k & <\xi\eta,\xi>_k & <\xi\eta,\eta>_k \\ <\eta^2,\xi^2>_k & <\eta^2,\xi\eta>_k & <\eta^2,\eta^2>_k & <\eta^2,\xi>_k & <\eta^2,\eta>_k \\ <\xi,\xi^2>_k & <\xi,\xi\eta>_k & <\xi,\eta^2>_k & <\xi,\xi>_k & <\xi,\eta>_k \\ <\eta,\xi^2>_k & <\eta,\xi\eta>_k & <\eta,\eta^2>_k & <\eta,\xi>_k & <\eta,\eta>_k \end{bmatrix} \qquad \mathbf{b} = \begin{bmatrix} <f,\xi^2>_k \\ <f,\xi\eta>_k \\ <f,\eta^2>_k \\ <f,\xi>_k \\ <f,\eta>_k \end{bmatrix} .$$

where $<\zeta,\gamma>_k = \sum_{k=1}^{m} W_k(\xi,\eta)\zeta_k\gamma_k$ and $W_k(\xi,\eta) = e^{-5\sqrt{\xi^2+\eta^2}}$ is the exponential weight function. Considering Eq. (9) it can be determined that

$$\left.\frac{\partial f}{\partial x}\right|_I = \left.\frac{\partial f}{\partial \xi}\right|_{\substack{\xi=0\\ \eta=0}} = c_4 \ , \qquad \left.\frac{\partial f}{\partial y}\right|_I = \left.\frac{\partial f}{\partial \eta}\right|_{\substack{\xi=0\\ \eta=0}} = c_5 \ , \qquad \left.\frac{\partial^2 f}{\partial x^2}\right|_I = \left.\frac{\partial^2 f}{\partial \xi^2}\right|_{\substack{\xi=0\\ \eta=0}} = 2c_1 \ ,$$
$$\left.\frac{\partial^2 f}{\partial y^2}\right|_I = \left.\frac{\partial^2 f}{\partial \eta^2}\right|_{\substack{\xi=0\\ \eta=0}} = 2c_3 \ , \quad \left.\frac{\partial^2 f}{\partial x \partial y}\right|_I = \left.\frac{\partial^2 f}{\partial \xi \partial \eta}\right|_{\substack{\xi=0\\ \eta=0}} = c_2 \ . \tag{11}$$

The derivatives found in Eq. (11) can be used to discretizate the governing equations. In the Finite Volumes method, the surface integral into momentum equation given by Eq. (2) is evaluated in the control volume of Fig. 1 a using:

$$\oint_S \left[\left(\frac{1}{Re}\frac{\partial u}{\partial x} - u^2\right)dy - \left(\frac{1}{Re}\frac{\partial u}{\partial y} - uv\right)dx\right] = \oint_S \left(\frac{1}{Re}\frac{\partial u}{\partial x} - u^2\right)dy - \oint_S \left(\frac{1}{Re}\frac{\partial u}{\partial y} - uv\right)dx \ . \tag{12}$$

Doing $E = \frac{1}{Re}\frac{\partial u}{\partial x} - u^2$ and $F = \frac{1}{Re}\frac{\partial u}{\partial y} - uv$ in Eq. (12) is had:

$$\oint_S Edy - \oint_S Fdx \qquad \text{when}$$
$$\left.\oint_S Edy\right|_{E_4} \approx \frac{1}{2}\left[(E_4 + E_1)dy_{ab} + (E_4 + E_2)dy_{bc} + (E_4 + E_3)dy_{cd}\right] \ ,$$
$$\left.\oint_S Fdx\right|_{E_4} \approx \frac{1}{2}\left[(F_4 + F_1)dx_{ab} + (F_4 + F_2)dx_{bc} + (F_4 + F_3)dx_{cd}\right] \ .$$

The derivative $\frac{\partial u}{\partial x}$ in Eq. (12) is approximated by

$$\left.\frac{\partial u}{\partial x}\right|_{E_4} \approx \frac{1}{V}\int_V \frac{\partial u}{\partial x}dV = \frac{1}{V}\oint_S udy \approx \frac{1}{2V}\left[(u_4 + u_1)dy_{ab} + (u_4 + u_2)dy_{bc} + (u_4 + u_3)dy_{cd}\right] \ .$$

For $\frac{\partial u}{\partial y}$ and points $E_1$, $E_2$ and $E_3$ the procedure is analogous. To solve the linear system, to find the pressure field, it was used the Bi-conjugated Gradient Stabilized procedure, according to Barret et al. (1994), in all methods. This method solves linear systems when the matrix is non-symmetric and non-positive definite. The flow is induced by the sliding motion of the top wall $y = 1$ from left to right and is described by the Navier-Stokes equations Eq. (1) and Eq. (2). The boundary conditions are those no-slip on the stationary walls $u = 0$ and $v = 0$, on the sliding wall $u = 1$ and $v = 0$ according to Fig. 1 b.

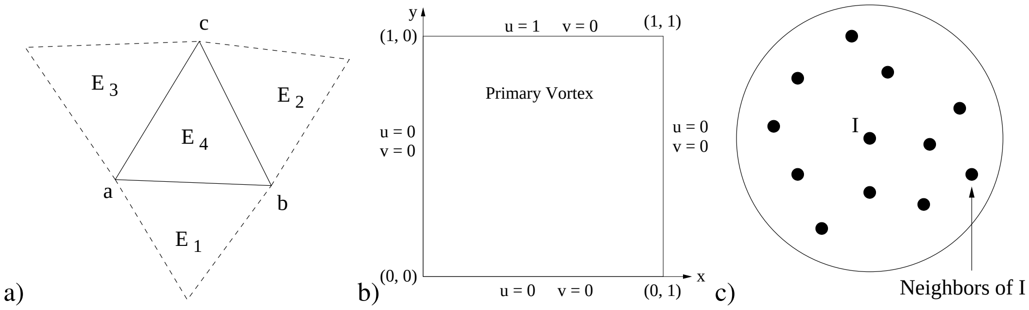


Figure 1. a) Finite Volumes Cell b) Cavity Problem c) Neighbors of I Point

## 3. Results

The results were obtained running the cavity problem to Meshless points showed in Fig. 2 a, unstructured Finite Volumes mesh according to Fig. 2 b and regular structured mesh, with 50x50 points, to Finite Differences method.

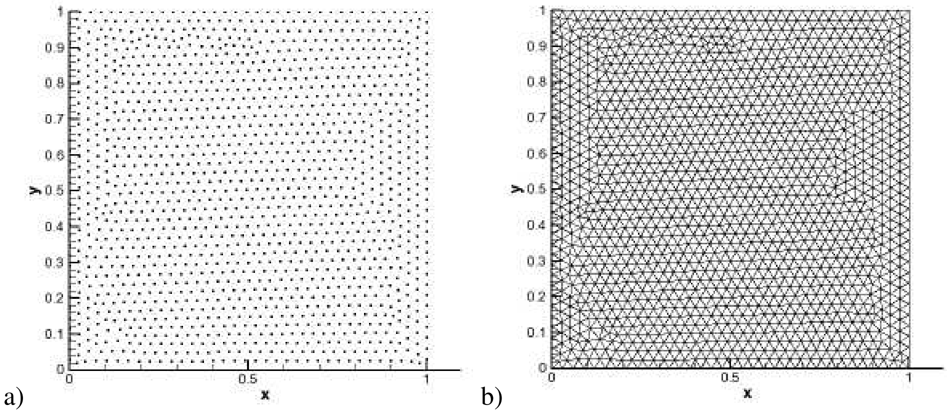


Figure 2. a) Meshless Points b) Finite Volumes Mesh

The streamlines for Finite Differences method are shown in Fig. 3 . The Fig. 4 shows the streamlines for Meshless method and the Fig. 5 shows the streamlines for Finite Volumes method. All cases using Reynolds number equal to $0.1$, $10$, $50$ and $100$. The graphics in Fig. 6 to Fig. 9 present the variation of the velocity components $u$ and $v$ along the vertical ($x = 0.5$) and horizontal ($y = 0.5$) lines, at various Reynolds numbers. The graphics in Fig. 6 to Fig. 9 was plotted using a nodes band around of cavity centerlines, because the nodes of unstructured mesh don't coincide with the nodes of structured mesh. This prevent interpolations. The Tab. 1 presents a comparative $u$ and $v$-velocity in horizontal centerline at y=0.5 for $Re = 100$ and the Tab. 2 presents a comparative $u$ and $v$-velocity in vertical centerline at x=0.5 for $Re = 100$.

## 4. Discussions and Conclusions

According to graphics showed in Fig. 6 to Fig. 9 it can be observed that the Finite Differences and Finite Volumes methods present results very closed. These results are in good agreement with Semeraro and Sameh (1991), Schneider and Maliska (2000) and others. The Meshless method presents an artificial dissipation that is more evident at low Reynolds numbers. In agreement with Belytschko et al. (1996), experiments indicate that Mesless formulation can provide higher accuracy in comparison with the standard re-meshing used with viscous scheme, but it can be observed in Fig. 3 to Fig. 5 that the Meshless method are not so precise in capture the vorticity in the bottom corners of the driven cavity. This problem is commonly associated with the corner and boundary conditions used, that create discontinuities in that points, Günter and Liu (1997) and Choe et al. (2001). When the value of Reynolds number increases the inadequacy of coarse meshes gradually becomes apparent. This would imply that the velocity distributions near the corners are sensitive to mesh size. The accuracy of the solution can be tested plotting the $u$-velocity and $v$-velocity profiles, according Fig. 6 to Fig. 9 . The results obtained in this study, and compared with others, Schreiber and Keller (1983), show more accuracy for the Finite Volumes method follow the Meshless (Tab. 1 and Tab. 2).

Table 1. Comparative $u$-velocity and $v$-velocity table in horizontal centerline at y=0.5 for $Re = 100$.

| | Finite Diferences | | Finite Volumes | | Meshless | |
|---|---|---|---|---|---|---|
| Position | $ux$ | $vx$ | $ux$ | $vx$ | $ux$ | $vx$ |
| 0.25 | -0.096871 | 0.178925 | -0.092850 | 0.174070 | -0.081806 | 0.151773 |
| 0.5 | -0.207203 | 0.0518048 | -0.206589 | 0.057071 | -0.180446 | 0.057445 |
| 0.75 | -0.211439 | -0.233569 | -0.210336 | -0.229064 | -0.190579 | -0.191401 |

Table 2. Comparative $u$-velocity and $v$-velocity table in vertical centerline at x=0.5 for $Re = 100$.

| | Finite Diferences | | Finite Volumes | | Meshless | |
|---|---|---|---|---|---|---|
| Position | $uy$ | $vy$ | $uy$ | $vy$ | $uy$ | $vy$ |
| 0.25 | -0.146992 | -0.00114387 | -0.141713 | 0.002462 | -0.119133 | 0.006843 |
| 0.5 | -0.207203 | 0.0518048 | -0.206329 | 0.058145 | -0.179992 | 0.057980 |
| 0.75 | 0.036096 | 0.108712 | 0.023795 | 0.119201 | 0.020259 | 0.120330 |

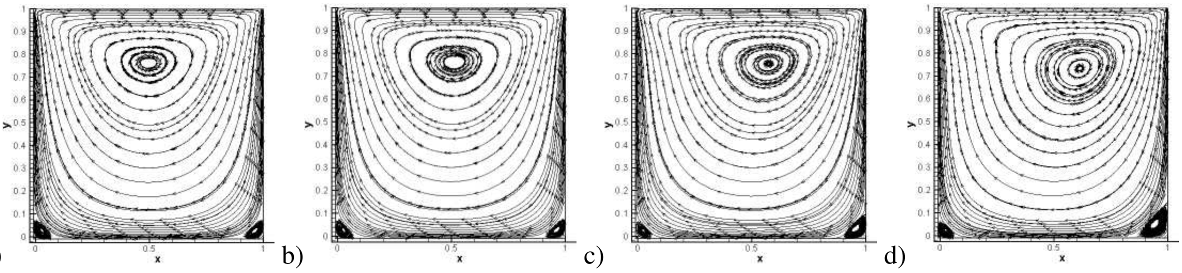

a) b) c) d)

Figure 3. Finite Differences: a)$Re = 0.1$ b)$Re = 10$ c)$Re = 50$ and d)$Re = 100$.

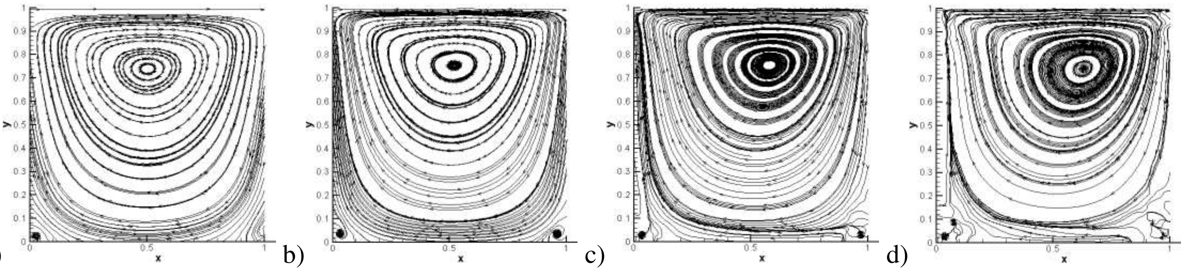

a) b) c) d)

Figure 4. Meshless: a)$Re = 0.1$ b)$Re = 10$ c)$Re = 50$ d)$Re = 100$.

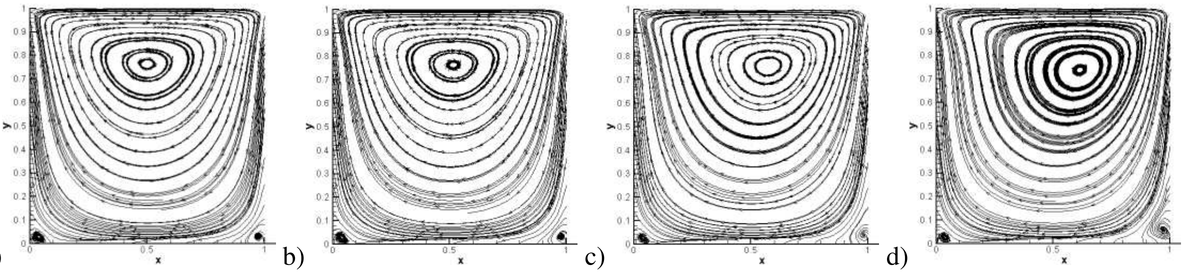

a) b) c) d)

Figure 5. Finite Volumes: a)$Re = 0.1$ b)$Re = 10$ c)$Re = 50$ d)$Re = 100$.

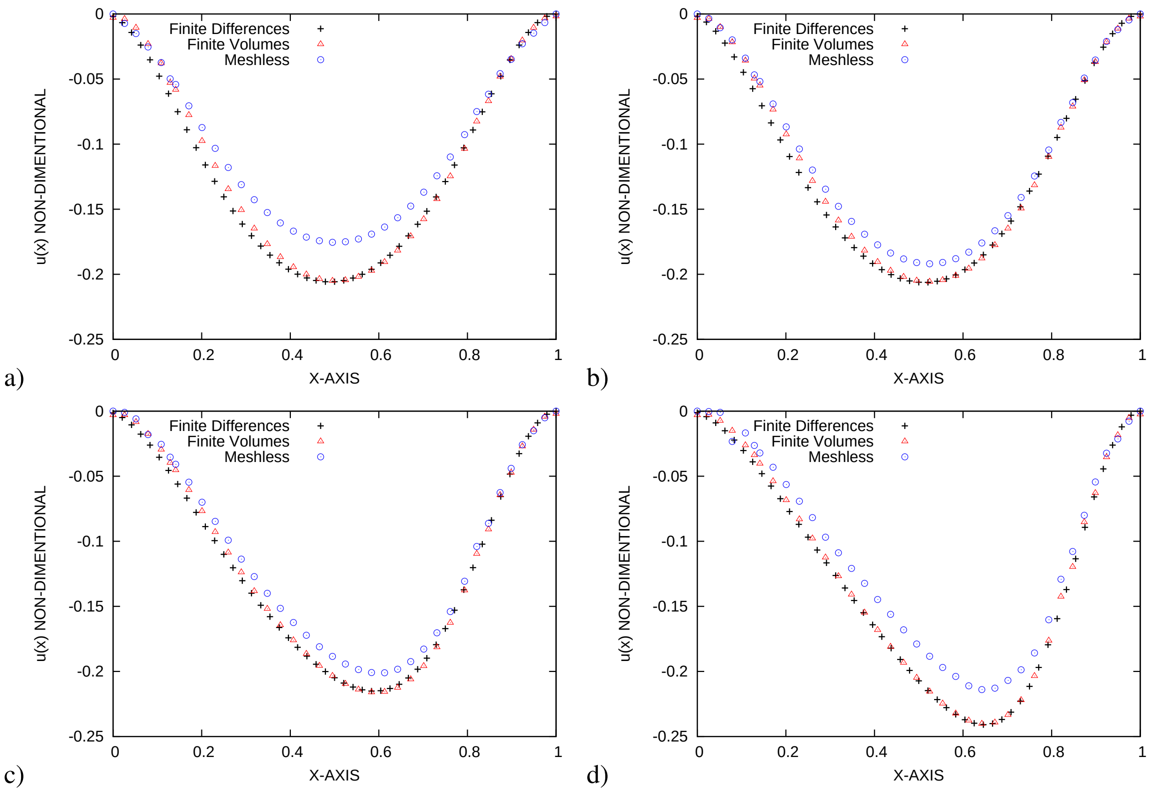


Figure 6. $u$ at $y = 0.5$: a)$Re = 0.1$ b)$Re = 10$ c)$Re = 50$ d)$Re = 100$.

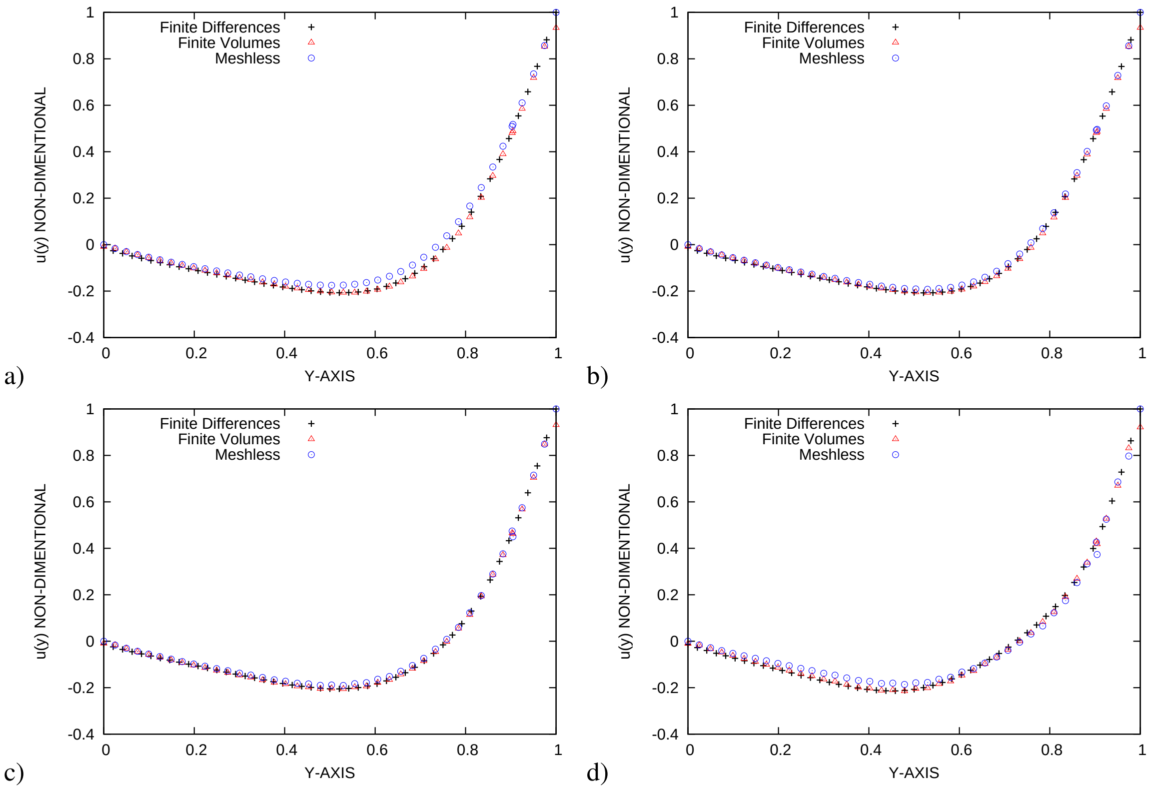


Figure 7. $u$ at $x = 0.5$: a)$Re = 0.1$ b)$Re = 10$ c)$Re = 50$ d)$Re = 100$.

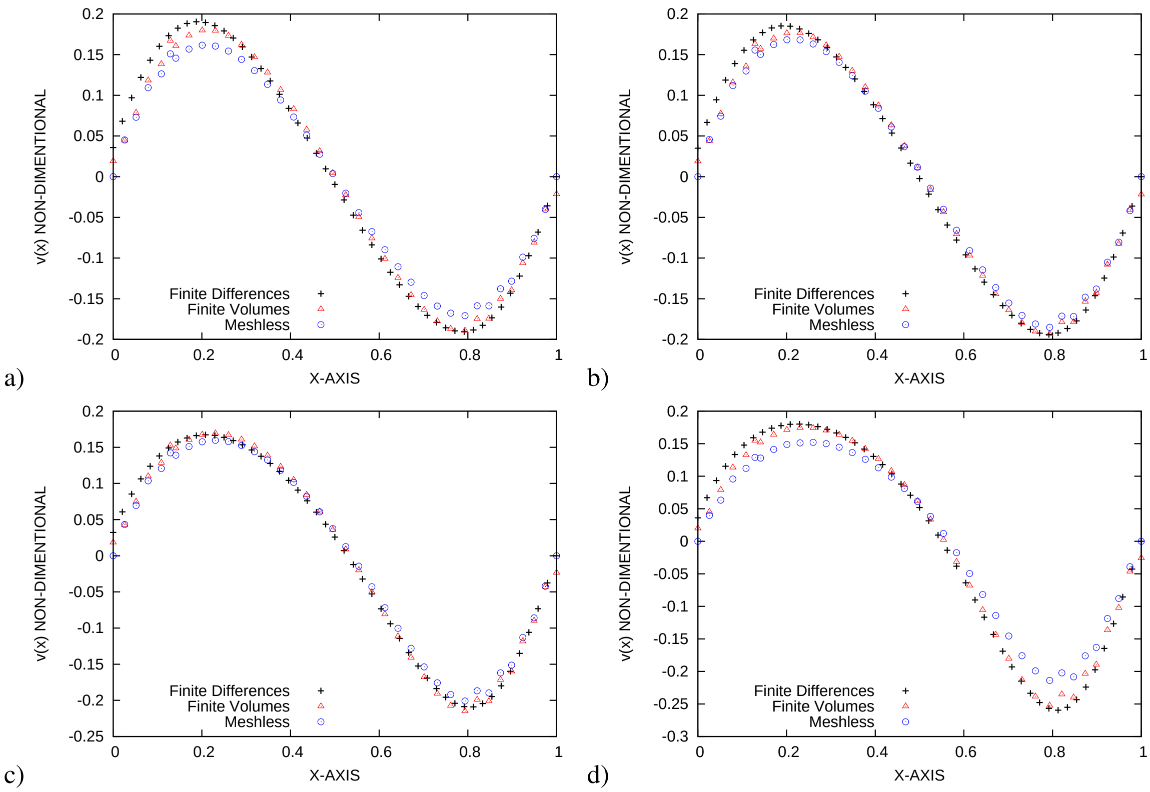


Figure 8. $v$ at $y = 0.5$: a)$Re = 0.1$ b)$Re = 10$ c)$Re = 50$ d)$Re = 100$.

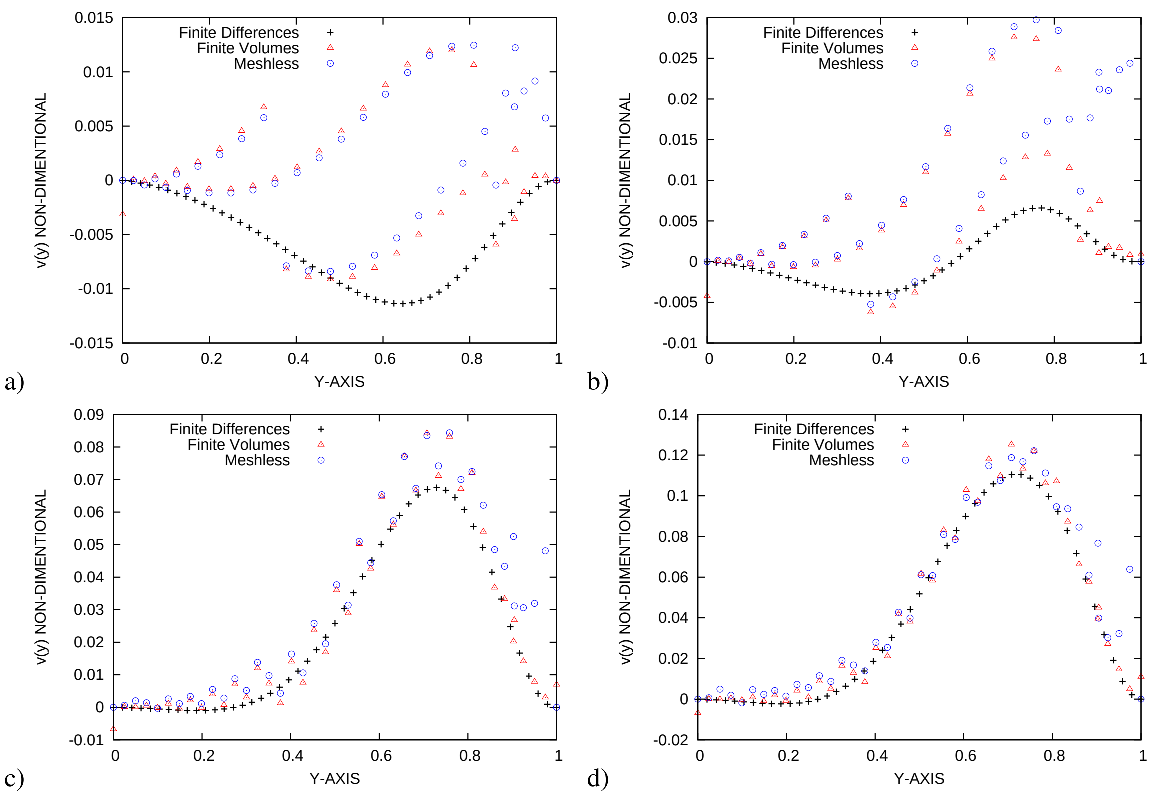


Figure 9. $v$ at $x = 0.5$: a)$Re = 0.1$ b)$Re = 10$ c)$Re = 50$ d)$Re = 100$.

The advantages or disadvantages of these numerical approaches and also numerical stability and any type of numerical issues are not our concern at the moment. For this, the discrepancies near the left and right hand of the corners of the cavity will be study with new strategies of boundary conditions and numerical approach. Considering the observations above, the present results are relevant and it's important to study this methods for meshes with more points near the boundary and few points in the center of cavity. Future effort includes consideration of primitive-variable formulation when applied for higher Reynolds numbers and unstructured mesh. Better computational times and quick solution will be possible with Multigrid techniques.

## 5. References

Barragy, E. and Carey, G. F. 1997. "Stream Function-Vorticity Driven Cavity Solutions using *p* Finite Elements". Computer and Fluids, 26:453–468.

Barret, R., Berry, M., Chan, T. F., Demmel, J., Donnato, J., Eijkhout, V., Pozzo, R., C, R., and der Vorst, H. V. 1994. "Templares for the solution of Linear Systems: Building Blocks for Iterative Methods". SIAM.

Belytschko, T., Krongaus, Y., Organ, D., Fleming, M., and Krysl, P. 1996. "Meshless methods: An Overview and Recent Developments". Computational Methods in Applied Mechanics Engeneering, 139:3–47.

Benjamin, A. S. and Denny, V. E. 1979. "On the Convergence of Numerical Solutions for 2-D Flows in a Cavity at Large Re". Journal of Computational Physics, 33:340–358.

Choe, H. J., Kim, D. W., Kim, H. H., and Kim, Y. 2001. "Meshless Method for the Stationary Incompressible Navier-Stokes Equations". Discrete And Continuous Dynamic Systems. Series B, 1(4):495–526.

Erturk, E., Corke, T. C., and Gakcol, C. 2004. "Numerical Solutions of 2-D Steady Incompressible Driven Cavity Flow at High Reynolds Number". International Journal of Numerical Methods in Fluids.

Fletcher, C. A. J. 1991. "Computational Techniques for Fluid Dynamics". Springer-Verlag, New York.

Ghia, U., Ghia, K. N., and Shin, C. T. 1982. "High-Re Solutions for the Incompressible Flow Using the Navier-Stokes Equations and a Multigrid Method". Journal of Computational Physics, 48:387–411.

Günter, F. C. and Liu, W. K. 1997. "Implementation of Boundary Conditions for Meshless Methods". Computer Methods in Applied Mechanics and Engineering.

Harlow, F. and Welch, J. E. 1965. "Numerical Calculation of Time-dependent Viscous Incompressible Flow of Fluid with a Free Surface". Phys. Fluids, 8:2182–2189.

Maliska, C. R. 2000. "Transferência de Calor e Mecânica dos Fluidos Computacional". LTC Editora, Rio de Janeiro.

Maliska, C. R. and Vasconcellos, J. F. V. 2000. "An Untructured Finite Volume Procedure for Simulating Flows with Moving Fronts". Computer Methods in Applied Mechanics and Engineering, pages 401–420.

Melenk, J. M. 1997. "On Approximation in Meshless Methods". ETH-Eidgenössische Technische Hochschule Zürich.

Schneider, F. A. and Maliska, C. R. 2000. "Uma Formulacão em Volumes Finitos usando Malhas Não-Estruturadas". VIII ENCIT - Encontro Nacional de Ciências Térmicas, CD Rom edition.

Schneider, F. A. and Maliska, C. R. 2002. "Solução Numérica Simultânea de Escoamentos Bidimensionais Incompressíveis pelo Método dos Volumes Finitos usando Malhas Não-estruturadas". ENCIT-9Th Brazilian Congress of Thermal Engineering and Sciences.

Schreiber, R. and Keller, H. B. 1983. "Driven Cavity Flows by Efficient Numerical Techniques". Journal of Computational Physics, 49:310–333.

Semeraro, B. D. and Sameh, A. 1991. "Solution of the Navier-Stokes Equations for a Driven Cavity". NASA-CR-188008 and Ilinois University.

Varonos, A. and Bergeles, G. 1998. "Development and Assessment of a Variable-order Non-oscillatory Scheme for Convection Term Discretization". International Journal of Numerical Methods in Fluids, 26:1–16.

Versteeg, H. K. and Malalasekera, W. 1995. "An Introduction to Computational Fluid Dynamics. The Finite Volume Method". Prentice Hall, Essex.

## 6. Responsibility notice

The authors are the only responsible for the printed material included in this paper.